

Effects of growing conditions on the electric and magnetic properties of strained
 $\text{La}_{2/3}\text{Sr}_{1/3}\text{MnO}_3$ thin films

This content has been downloaded from IOPscience. Please scroll down to see the full text.

2015 Chinese Phys. B 24 027504

(<http://iopscience.iop.org/1674-1056/24/2/027504>)

View [the table of contents for this issue](#), or go to the [journal homepage](#) for more

Download details:

IP Address: 159.226.35.189

This content was downloaded on 10/12/2015 at 15:03

Please note that [terms and conditions apply](#).

Effects of growing conditions on the electric and magnetic properties of strained $\text{La}_{2/3}\text{Sr}_{1/3}\text{MnO}_3$ thin films*

Lu Hai-Xia(卢海霞), Wang Jing(王晶), Shen Bao-Gen(沈保根), and Sun Ji-Rong(孙继荣)[†]

Beijing National Laboratory for Condensed Matter Physics and the Institute of Physics, Chinese Academy of Sciences, Beijing 100190, China

(Received 19 August 2014; revised manuscript received 14 October 2014; published online 10 December 2014)

We investigate the growing condition dependences of magnetic and electric properties of the $\text{La}_{2/3}\text{Sr}_{1/3}\text{MnO}_3$ thin films grown on SrTiO_3 (001) substrates. With reducing the film thickness and growth pressure, the Curie temperature (T_C) drops off, and the magnetism and metallicity are suppressed. At an appropriate deposition temperature, we can obtain the best texture and remarkably enhance the magnetic and electrical properties. However, the resistivity of film cannot be modulated by changing the dc current and green light intensity. This result may be induced by the coherent strains in the epitaxially grown film due to its lattice mismatching that of the SrTiO_3 substrate. Furthermore, we show that the relations between the magnetism and the resistivity for the typical films with different thickness values. For the 13.4-nm-thick film, the R - T curve presents two transition behaviors: insulator-to-metal and metal-to-insulator in the cooling process: the former corresponds to magnetic transition, and the later correlates with thermal excitation conduction.

Keywords: growing condition, magnetism, resistivity

PACS: 75.70.Ak, 68.55.A-, 75.47.Lx

DOI: 10.1088/1674-1056/24/2/027504

1. Introduction

Manganite-doped perovskites exhibit tantalizing magnetotransport properties, such as colossal magnetoresistance and half-metallicity,^[1,2] which make them very promising for spin valves or spin injectors.^[3–5] Most of the doped manganites present a magnetic transition at the Curie temperature T_C , accompanied by a metal–insulator transition, which converts them into paramagnetic insulators at high temperature and ferromagnetic half-metals at low temperature.^[6,7] $\text{La}_{2/3}\text{Sr}_{1/3}\text{MnO}_3$ (LSMO) is one of the intensively studied manganites, because it has the largest single electron bandwidth and the highest Curie temperature in the family of manganites ($T_C \sim 369$ K).^[1,2] A larger number of studies have proved the fabrication of such manganites in the forms of thin films, which show very different properties compared with the bulk. Recently, it has been reported that ultrathin films of LSMO with thickness values on the order of several nanometers may act as the “dead layers” with insulating behavior and depressed magnetization.^[5,8–12] A so-called “dead layer” thickness can be defined as the thinnest layer for which metallic and ferromagnetic behavior are observed.^[6] Although most of the studies on ultrathin LSMO films commonly focus on estimating the dead layer thickness values for LSMO films on the substrates of NdGaO_3 (110), MgO (001), and LaAlO_3 (001), etc., the material properties of LSMO films depend strongly on the growth mode and oxidation level, especially, only a slight variation in each of them can lead to the change of the electric and magnetic properties of the LSMO

films,^[8,10,11] which are relatively little researched.

In this work, we report the electrical transport and magnetic properties of the $\text{La}_{2/3}\text{Sr}_{1/3}\text{MnO}_3/\text{SrTiO}_3$ (100) films, and discuss the influences of the growth conditions, such as growing temperature, growing pressure, and the effect of the measurement methods, for example, the applied dc current and the green light, on the properties of the sample. Taking the 13.4-nm LSMO film as a representative sample, the separate regions can be distinguished in the transport behavior. At lower temperature, the sample transits to the insulating phase once again. These results are explained by considering the thermally activated conductivity.

2. Experiment

The films used in this study were grown epitaxially, using pulsed-laser deposition from a stoichiometric $\text{La}_{2/3}\text{Sr}_{1/3}\text{MnO}_3$ target, on SrTiO_3 (100) substrates by applying a 248-nm KrF excimer laser at a repetition rate of 1 Hz and a laser fluence of ~ 1.5 J/cm². We designed three different growing processes as shown in Table 1. The surface morphology was measured by an atomic force microscope (AFM) (Nanonavi E-Sweep) with a Si tip at room temperature. A Quantum Design superconducting quantum interference device (SQUID) measurement system was used to measure the magnetic properties in the temperature range 20 K–380 K with the magnetic field applied in-plane along the (100) direction of the SrTiO_3 crystal. The diamagnetic contributions from the substrate and the sample holders were measured and sub-

*Project supported by the National Natural Science Foundation of China (Grant Nos. 111374348, 11134007, 11174345, and 111474341) and the National Basic Research Program of China (Grant Nos. 2013CB921700, 2011CB921801, and 2012CB933000).

[†]Corresponding author. E-mail: jrsun@iphy.ac.cn

tracted from the data. The electrical resistance was obtained with a Cycle Refrigeration system through different contact configurations: a standard four-probe configuration for dc current measurements using a Keithley 2601 SourceMeter and 2182 Nanovoltmeter, and a two-probe scheme for dc voltage measurement using a Keithley 6517B electrometer.

3. Results and discussion

In Table 1 we present the values of the growing temperature and growing pressure for the different films. Also included in Table 1 are the three comparison procedures. (i) The growing times are the same and the substrates are held at 750 °C in an oxygen environment in the pressure range 4×10^{-4} mbar– 5×10^{-3} mbar (1 bar = 10^5 Pa). (ii) The growing times are different and the substrate is kept at 750 °C in an unchanged oxygen environment of 1×10^{-3} mbar. (iii) The growing times and pressures are the same, the substrate tem-

perature varies in a range of 750 °C–800 °C.

Figures 1(a)–1(c) show the AFM micrographs of the 2#, 3#, and 4# films in an area of $2 \mu\text{m} \times 2 \mu\text{m}$, respectively. The images show the different growth modes from the layer-by-layer growth to island growth with the deposition pressure increasing. The calculated root-mean-square roughness values of the film increase with increasing the growth pressure, which are about 1 Å, 2 Å, and 5 Å, correspondingly. That is to say, the lower growing pressure is more conducive to the formation of the smooth surface. Simultaneously, compared with the other growing temperatures,^[10] the appropriate deposition temperature can obtain the best texture as shown in Fig. 1(d). The figure shows the AFM micrograph of the 5# film and a line scan result (along the arrow direction). The peak-to-valley roughness of the film is less than 2 Å. The calculated root-mean-square roughness of the film is about 1 Å, which is smaller than the film thickness.

Table 1. Values of growing temperature and growing pressure for the different $\text{La}_{2/3}\text{Sr}_{1/3}\text{MnO}_3$ (LSMO) films.

Procedure	(i)			(ii)			(iii)	
	2#	3#	4#	1#	2#	6#	3#	5#
Growing pressure/ 10^{-3} mbar	1	5	0.4	1	1	1	1	1
Growing temperature/°C	750	750	750	750	750	750	750	800
Film thickness/nm	13.4	12.9	13	6	13.4	26.8	12.9	13

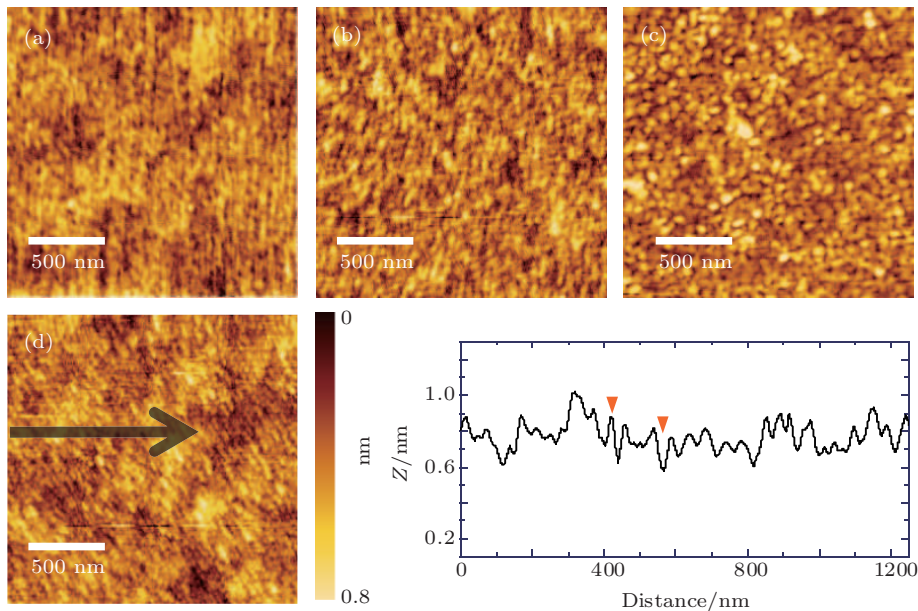


Fig. 1. (color online) ((a)–(c)) Typical AFM micrographs of 2#, 3#, and 4# LSMO films epitaxially grown on (100) SrTiO_3 substrates. (d) The AFM micrograph of the 5# film and a line scan result (along the arrow direction).

Figure 2(a) shows the temperature dependences of the magnetization with an in-plane magnetic field of 500 Oe ($1 \text{ Oe} = 79.5775 \text{ A} \cdot \text{m}^{-1}$ for six LSMO films. Each of all the films undergoes a ferromagnetic-to-paramagnetic transi-

tion with increasing the temperature from 20 K to 380 K. As expected, the T_C values of the films increase as the growth pressure and thickness values of the films augment. Figure 2(b) shows clear ferromagnetic hysteresis loops for the dif-

ferent samples at 20 K. The large differences in the saturation magnetization value can be observed, for LSMO films grown at pressures from 4×10^{-4} mbar to 5×10^{-3} mbar, to lead to magnetizations in the range of 150 emu/cm^3 – 230 emu/cm^3 (see the inset of Fig. 2(b)), and the thinnest film (6 nm) exhibits a drastically reduced magnetization of $\sim 40 \text{ emu/cm}^3$. These results indicate that oxygen deficiencies are responsible for the reduced magnetization but do not affect the surface roughness, however, both of them can be influenced by film thickness. Although LSMO growth at lower pressure shows the smoothest surface, it has inferior magnetic properties when

compared with films grown at higher pressure.^[6] The dependences of the coercive field H_C and the Curie temperature T_C on the thickness and growth pressure are shown in Figs. 2(c) and 2(d), respectively. The coercive field H_C is nearly constant for the thickness and the growth pressure, based on the results reported by Ramesh *et al.*,^[6] further reducing the film thickness and the growth pressure results in a dramatic change in magnetic property. The Curie temperature T_C is lowered with reducing the thickness and the growth pressure. So, the selection of the appropriate growing condition is the matter of greatest concern.

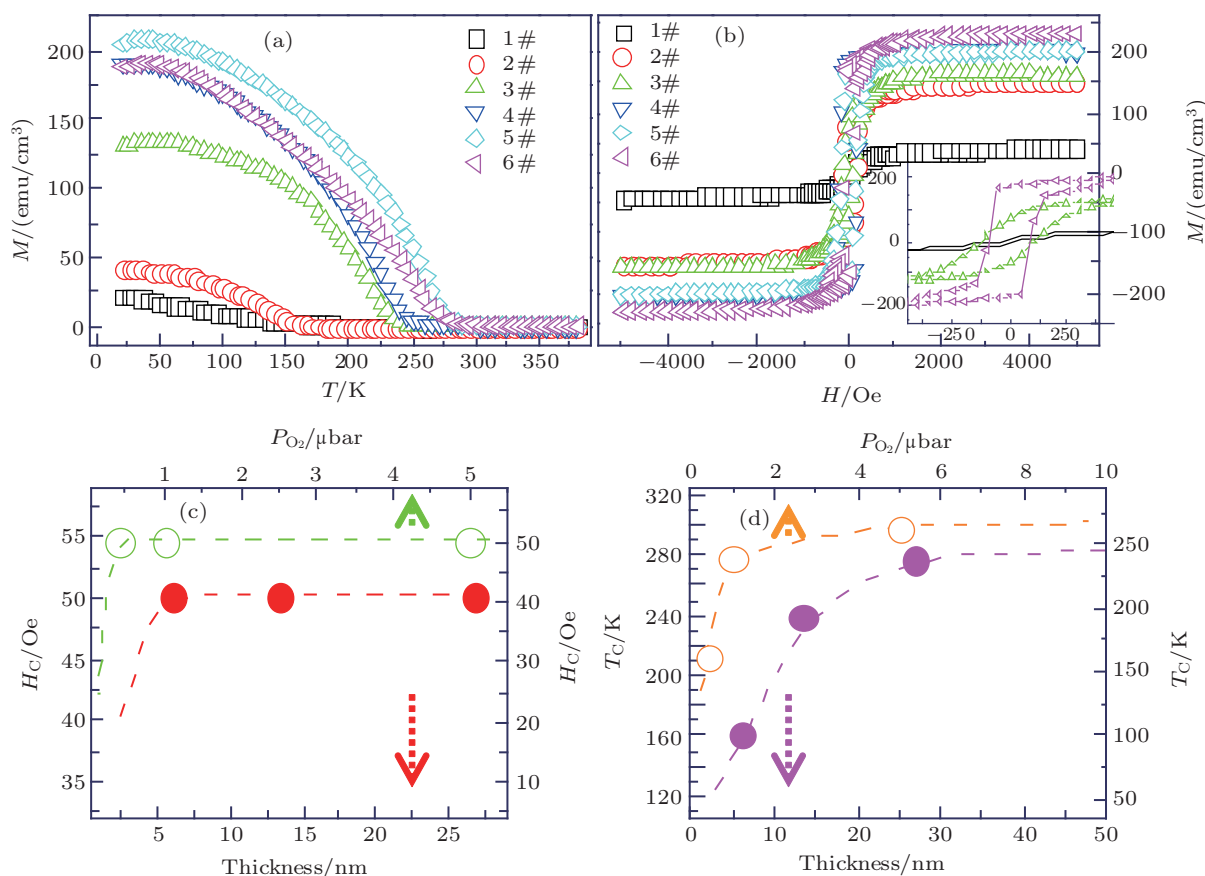


Fig. 2. (color online) Magnetic properties of the LSMO films on SrTiO₃ (100) grown under different growing conditions, showing (a) temperature dependences of the magnetization measured at 500 Oe, (b) magnetic hysteresis loops measured at 20 K and the enlarged hysteresis loops of the 1#, 3#, and 6# films near the origin, (c) the dependences of coercive field H_C on the thickness and growth pressure, and (d) the dependences of Curie temperature T_C on the thickness and growth pressure. (The dashed curves represent the fitted curves on the basis of the results reported in the literature.)

The temperature dependences of the resistivity in zero magnetic field for the LSMO films with varying thickness, growing pressure, deposition temperature, applied dc current, and green light intensity are given in Figs. 3(a)–3(d), respectively. Figure 3(a) shows the R – T curves of LSMO films grown at a pressure of 1×10^{-3} mbar with three different thickness values. The transport behavior of 6-nm film is insulating in the whole temperature range, while the resistivity of the 23.8-nm film shows a bulk-like metallic behavior over the

whole temperature regime. For the LSMO films with thickness values of 26.8, 13.4, and 6 nm, a continuous resistivity increase is observed obviously to rise by more than 3 orders in magnitude, which indicates the presence of a layer with great conductivity in the thickest film. However, due to the lower growth pressure, this layer is relatively thick compared with other reported one.^[6] As shown in Fig. 3(b), the temperature dependence of resistance for 13-nm film of increasing growth pressure presents a similar change tendency to that of

the magnetic properties. These results together with the magnetic properties again demonstrate that the oxygen deficiencies are responsible for the reduced resistivity and magnetization.

In Fig. 3(c) we present the variations of resistivity with temperature for the different films that are deposited at the following two substrate temperatures: 750 °C and 800 °C. It is remarkable that the transport behaviors of the films deposited at 750 °C and 800 °C are insulating and metallic in the whole temperature range, respectively. These results indicate that the films' quality and properties are strongly dependent on the

substrate temperature during deposition.^[10] Figure 3(d) shows the temperature dependence of resistivity measured by using the four probe method under different dc currents and green light intensities, however, the R - T curves cannot be modulated by different dc currents and green light intensities. This is in strong contrast to the situation of LSMO films grown on LaAlO₃.^[13–16] We believe that the major difference between the films discussed here and the films on LaAlO₃ lies in their different strain states: coherently strained on SrTiO₃ and fully relaxed on LaAlO₃.^[12]

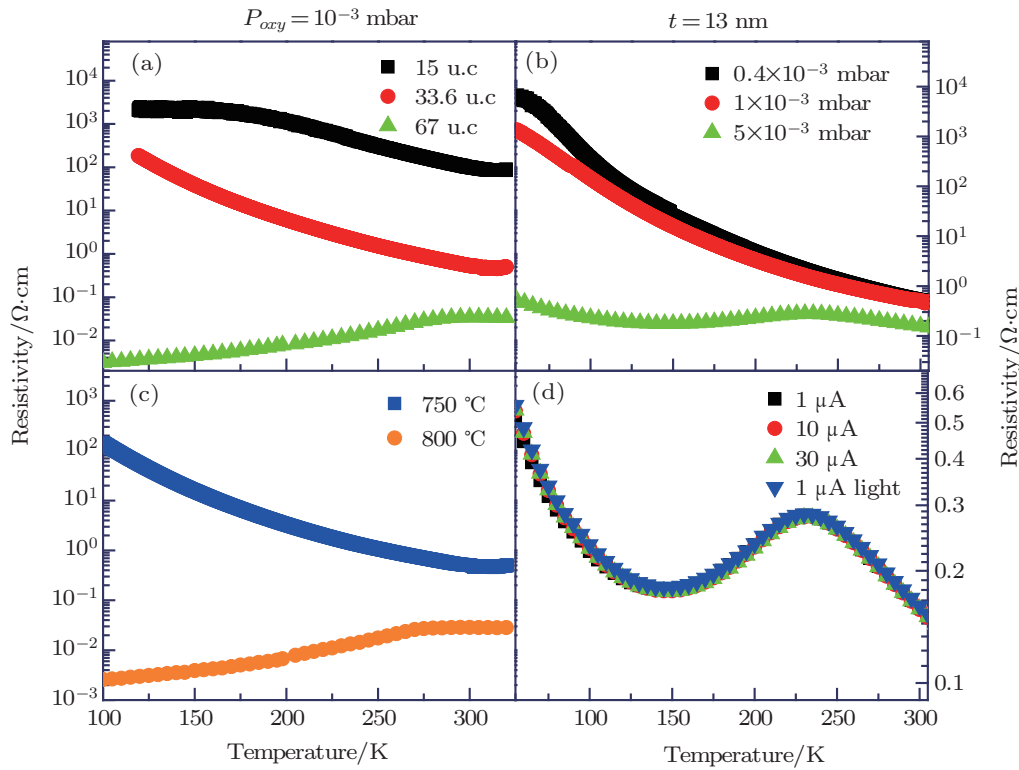


Fig. 3. (color online) Transport behaviors of the LSMO films on SrTiO₃(100) substrates, showing (a) the R - T curves of LSMO films grown at a pressure of 1×10^{-3} mbar with three different thickness values, (b) the temperature dependences of resistances for 13-nm films at three different pressures, (c) resistivities of the films deposited at two different substrate temperatures versus pressure. (d) The temperature dependences of resistivities for various dc current and green light intensities. (The films in panels (a) and (c) are deposited at the same pressure 1×10^{-3} mbar. The films in panels (b) and (d) have the same thickness value of 13 nm).

Figures 4(a)–4(c) show the correlations of transport behavior and magnetic properties of La_{2/3}Sr_{1/3}MnO₃ films grown at 1×10^{-3} mbar for three different thickness values of 6, 13.4, and 26.8 nm respectively. For the 26.8-nm film, the temperature of metal-to-insulator transition T_p is consistent with the Curie temperature (T_C).^[17] Such a behavior indicates the stronger coupling between ferromagnetism and metallicity.^[10] For the thinner (6 nm) film, the magnetic transition leads to the fact that the R - T curves each present a break point at about 150 K (T_b). The film is insulating in the whole temperature range, therefore, the transition is only from one nonmagnetic insulator to another magnetic insulator upon cooling. For 13.4-nm film grown at $P = 5 \times 10^{-3}$ mbar, the R - T curve of the film presents a two-transition behav-

ior: insulator-to-metal (T_1) and metal-to-insulator (T_2) in the cooling process, and a similar transition also emerges on the LSAT substrate.^[18] Maybe this thickness approaches to the dead layer thickness, while the transport behavior begins to present the insulator-to-metal transition just like the first transition. This transition is correlated with the paramagnetic-ferromagnetic transition, which produces a maximum in the resistivity near T_C ; however, the second transition shows that the film enters into the insulating phase once again, and the resistivity increases with the decrease of temperature. Kim *et al.* inferred the stronger magnetism of the better conductivity for the La_{2/3}Sr_{1/3}MnO₃ films.^[18] Although the magnetism can strengthen the conductivity, it does not prevent the tendency from entering into the insulating phase at low temper-

ature. That is to say, there are other factors that affect the films. Based on the magnetic and electrical properties of the $\text{La}_{2/3}\text{Sr}_{1/3}\text{MnO}_3$ film at low temperature, the carriers of the film can be localized. Localized carriers may induce the film transition from metal to insulator. The $\ln \rho \sim T^{-1}$ curve of

the 13.4-nm film is shown in Fig. 4(d). It is found that this curve can be fitted at the low temperature using the Arrhenius equation^[19,20] for the resistivity ρ at temperature T . This result indicates that the insulating phase may be induced through thermionic excitation at low temperature.

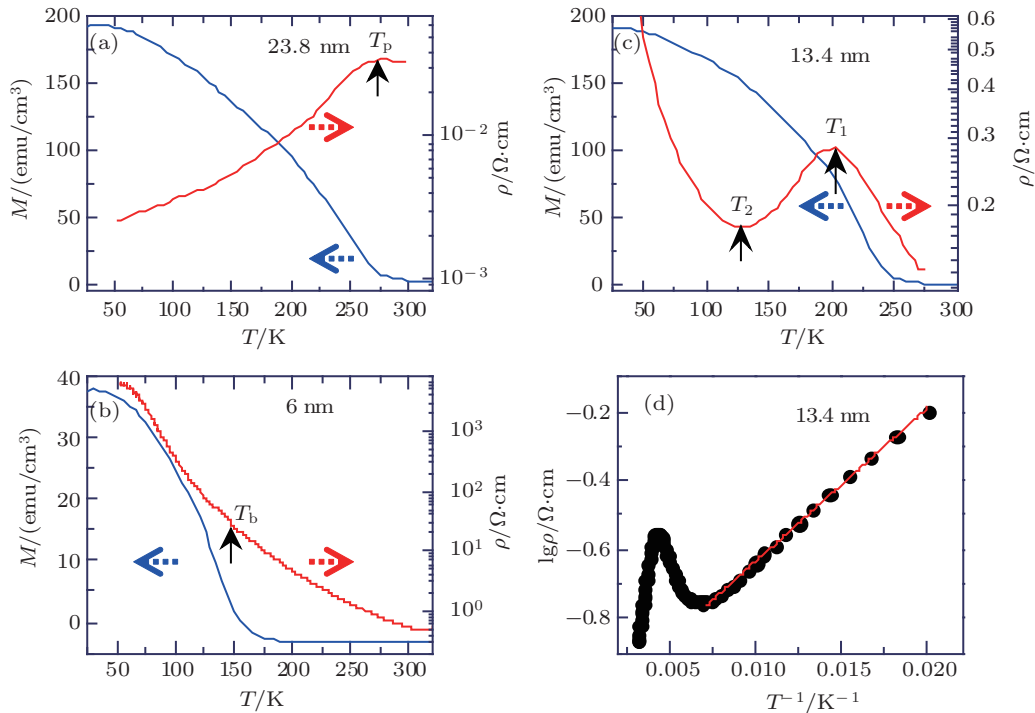


Fig. 4. (color online) (a)–(c) Correlations of the paramagnetic–ferromagnetic transition and the metal–insulator transition. (d) The black curve is the $\ln \rho \sim T^{-1}$ curve of the 13.4-nm film. The red line represents the fitted line on the basis of the Arrhenius equation at low temperature.

4. Conclusions

Detailed investigations of the LSMO films, where the film thickness, the growth pressure, and the deposited temperature can control the surface morphology and the magnetoelectricity, demonstrate the depressing of the magnetism and metallicity and the declining of the Curie temperature (T_C) with reducing the film thickness and growth pressure. Particularly, both the dc current and green light intensity cannot influence the electrical transport. This result may be induced by the coherent strain from SrTiO_3 substrate. Interestingly, a typical thickness of 13.4-nm film presents a two-transition process on the R – T curve. They are corresponding to magnetic transition and the thermionic activation, respectively.

References

- [1] Coey J D, Viret M and Von Molnár S 1999 *Ads. Phys.* **48** 167
- [2] Urushibara A, Moritomo Y, Arima T, Asamitsu A, Kido G and Tokura Y 1996 *Phys. Rev. B* **51** 14103
- [3] Marie-Bernadette L, Bernard M and Charles S 2012 *Phys. Rev. Lett.* **108** 087202
- [4] Tsui F, Smoak M C, Nath T K and Eom C B 2000 *Appl. Phys. Lett.* **76** 2421
- [5] Ziese M, Semmelhack H C and Han K H 2003 *Phys. Rev. B* **68** 134444
- [6] Huijben M, Martin L W, Chu Y H, Holcomb M B, Yu P, Rijnders G, Blank D H A and Ramesh R 2008 *Phys. Rev. B* **78** 094423
- [7] Fang Z, Solovyev I V and Terakura K 2000 *Phys. Rev. Lett.* **84** 3169
- [8] Sun J Z, Abraham D W, Rao R A and Eom C B 1999 *Appl. Phys. Lett.* **74** 3017
- [9] Bibes M, Valencia S, Balcells L, Martínez B, Fontcuberta J, Wojcik M, Nadolski S and Jedryka E 2002 *Phys. Rev. B* **66** 134416
- [10] Borges R P, Guichard W, Lunney J G, Coey J M D and Ott F 2001 *J. Appl. Phys.* **89** 3868
- [11] Angeloni M, Balestrino G, Boggio N, Medaglia P G, Orgiani P and Tebano A 2004 *J. Appl. Phys.* **96** 6387
- [12] Ziese M, Semmelhack H C, Han K H, Sena S P and Blythe H J 2002 *J. Appl. Phys.* **91** 3868
- [13] Sun Y H, Zhao Y G, Zhu M H, Xie B T and Wu W B 2012 *J. Appl. Phys.* **112** 023908
- [14] Sun Y H, Zhao Y G, Tian H F, Xiong C M, Xie B T and Zhu M H 2008 *Phys. Rev. B* **78** 024412
- [15] Sun J R, Liu G J, Zhang S Y, Han X F and Shen B G 2005 *Appl. Phys. Lett.* **86** 242507
- [16] Xie Y W, Sun J R, Wang D J, Liang S, Lu W M and Shen B G 2006 *Appl. Phys. Lett.* **89** 172507
- [17] Zener C 1951 *Phys. Rev. B* **82** 403
- [18] Kim B, Kwon D, Yajima T, Bell C H, Hikita Y, Kim B G and Hwang H Y 2011 *Appl. Phys. Lett.* **99** 092513
- [19] Xue Z Q, Huang S R, Zhang B P and Chen C 2010 *Acta Phys. Sin.* **59** 5002 (in Chinese)
- [20] Zhao N, Huang M L, Ma H T, Pan X M and Liu X Y 2013 *Acta Phys. Sin.* **62** 086601 (in Chinese)